Bulletin of the Seismological Society of America, Vol. 96, No. 4B, pp. S206–S220, September 2006, doi: 10.1785/0120050810

Seismomagnetic Effects from the Long-Awaited 28 September 2004 **M** 6.0 Parkfield Earthquake

by M. J. S. Johnston, Y. Sasai, G. D. Egbert, and R. J. Mueller

Abstract Precise measurements of local magnetic fields have been obtained with a differentially connected array of seven synchronized proton magnetometers located along 60 km of the locked-to-creeping transition region of the San Andreas fault at Parkfield, California, since 1976. The **M** 6.0 Parkfield earthquake on 28 September 2004, occurred within this array and generated coseismic magnetic field changes of between 0.2 and 0.5 nT at five sites in the network. No preseismic magnetic field changes exceeding background noise levels are apparent in the magnetic data during the month, week, and days before the earthquake (or expected in light of the absence of measurable precursive deformation, seismicity, or pore pressure changes). Observations of electric and magnetic fields from 0.01 to 20 Hz are also made at one site near the end of the earthquake rupture and corrected for common-mode signals from the ionosphere/magnetosphere using a second site some 115 km to the northwest along the fault. These magnetic data show no indications of unusual noise before the earthquake in the ULF band (0.01–20 Hz) as suggested may have preceded the 1989 M_L 7.1 Loma Prieta earthquake. Nor do we see electric field changes similar to those suggested to occur before earthquakes of this magnitude from data in Greece. Uniform and variable slip piezomagnetic models of the earthquake, derived from strain, displacement, and seismic data, generate magnetic field perturbations that are consistent with those observed by the magnetometer array. A higher rate of longer-term magnetic field change, consistent with increased loading in the region, is apparent since 1993. This accompanied an increased rate of secular shear strain observed on a two-color EDM network and a small network of borehole tensor strainmeters and increased seismicity dominated by three **M** 4.5–5 earthquakes roughly a year apart in 1992, 1993, and 1994. Models incorporating all of these data indicate increased slip at depth in the region, and this may have played a role in the final occurrence of the 28 September 2004 **M** 6.0 Parkfield earthquake. The absence of electric and magnetic field precursors for this, and other earthquakes with **M** 5–7.3 elsewhere in the San Andreas fault system, indicates useful prediction of damaging earthquakes seems unlikely using these electromagnetic data.

Introduction

Time-dependent local magnetic anomalies have been expected and detected as a result of stress changes that accompany seismic fault failure (Sasai, 1980, 1991; Stacey, 1964; Stacey and Johnston, 1972) Magnetic field changes (usually termed tectonomagnetic effects [TMEs] for effects related to aseismic tectonic activity and seismomagnetic effects [SMEs] for effects related to earthquakes) were observed to accompany the 8 July 1986 **M** 5.9 North Palm Springs earthquake (Johnston and Mueller, 1987), the 18 October 1989 M_L 7.1 Loma Prieta earthquake (Mueller and Johnston, 1990), and the 28 June 1992 **M** 7.3 Landers earthquake (Johnston *et al.*, 1994). These observations are readily explained in terms of piezomagnetic changes in crustal rocks expected on the basis of stress changes calculated from geodetic and seismologic models of these earthquakes. It seems that seismomagnetic effects are a normal feature of earthquakes with **M** $>$ 6.0.

Detection of local magnetic changes preceding earthquakes of this magnitude is much less clear (Johnston, 1989; Park *et al.*, 1993). No indications of precursory magnetic field changes are apparent in data from at least two independent near-field magnetometers in our continuous array along the San Andreas fault for some 150 or so earthquakes with **M** $>$ 5.0 in the last 25 years. We have just one case of a

clear 1 nT anomaly seen before a nearby **M** 5.2 earthquake on a single instrument (Smith and Johnston, 1976) with some indications of the same anomalous signal at a second site (Davis *et al.*, 1980).

Low-frequency (0.01–10 Hz) (usually termed ULF) and high-frequency (80 KHz) magnetic noise has recently been suggested to precede earthquakes. In particular, ULF signals were suggested to precede the 12 July 1988 **M** 6.8 Spitak, Armenia, earthquake (Kopytenko *et al.*, 1993), the 18 October 1989 M_L 7.1 Loma Prieta earthquake (Fraser-Smith *et al.*, 1990), and the 8 August 1993 **M** 8 Guam earthquake (Hayakawa *et al.*, 1996). Unfortunately, all of these observations were made on single instruments with no correction for ionospheric and magnetospheric noise. More serious problems are the lack of reproducibility of these signals, the absence of corresponding (larger) signals coincident with these earthquakes when the major energy release is occurring, and clear indications that these signals relate to earthquake source parameters. Signals similar to those seen on a single magnetometer by Fraser-Smith *et al.* (1990) preceding the Loma Prieta earthquake were not observed on a small array of magnetometers following the 1999 **M** 7.1 Hector Mine earthquake (Karakelian *et al.*, 2002). Similar signals were also not seen at the time of the 17 January 1994 **M** 6.7 Northridge earthquake (Fraser-Smith *et al.*, 1994). Nonetheless, based on the possibility that these magnetic signals might be earthquake related, many experiments are being implemented worldwide to search for these effects (e.g., Hayakawa, 1999), including many involving the use of satellites for rapid worldwide detection of these signals (Parrot, 1994).

Increased, though controversial, interest in tectonoelectric (TE) phenomena related to earthquakes has also occurred recently, primarily as a result of suggestions in Greece and Japan that short-term geoelectric field transients (seismoelectric signals [SESs]) of particular form and character precede earthquakes with magnitudes greater than 5 at distances up to several hundreds of kilometers (Varotsos *et al.*, 1993a, b; Nagao *et al.*, 1996). Controversy about these results exists because (1) there are no similar coseismic signals observed when the primary earthquake energy is released that can be causally related to the earthquake source, (2) no clear physical explanation exists describing how the SES signals can relate to earthquakes occurring sometimes hundreds of kilometers away (Bernard, 1992), (3) no independent data (strain, seismic, pore pressure, etc.) exists that supports the proposed earthquake/SES relationship, and (4) the SES signals have the form expected from rectification/saturation effects of local radio transmissions from high-power transmitters on nearby military bases (Pham *et al.*, 1998). The PK site in Parkfield has multiple electrodes, and peak-to-peak noise in data corrected for background disturbance is less than 20 μV/km, many orders of magnitude below that reported from the Greek SES measurements. The EM experiment thus provides an ideal test for these SES signals, particularly since the electrodes are much closer to the earthquake rupture and the earthquake magnitudes are comparable.

The 28 September 2004 **M** 6.0 Parkfield earthquake thus offers a unique new opportunity to identify each of these different magnetic and electric field changes before, during, and following the earthquake. Its epicenter was within the 50-km locked-to-creeping transition segment of the San Andreas fault where **M** 6.0 earthquakes have occurred in quasiperiodic manner from 1881 to the present (Langbein *et al.*, 2005). Electric and magnetic field monitoring instrumentation surrounding the earthquake includes a time-synchronized network of seven absolute magnetometers (Mueller *et al.*, 1981), a large-scale electric field monitoring array (Park, 1997), and a bandlimited (0.001–10 Hz) magnetic and electric (EM) field monitoring site at the northern end of the rupture (Egbert *et al.*, 2000). This EM experiment fortunately covers the ULF band commonly reported to exhibit disturbance before earthquakes. Numerous other displacement, strain, velocity, acceleration, pore pressure, and other data also exist to provide independent constraints on physical processes that might be occurring in concert with any magnetic field and electric changes. The earthquake thus provides the best multiparameter data yet available to determine the reality of magnetic and electric field changes related to earthquakes.

The location of the mainshock rupture in relation to the main trace and southwest trace of the San Andreas fault at Parkfield is shown in Figure 1. Seismic and geodetic moment tensor inversion (Chen *et al.*, 2004; Dreger *et al.*, 2004; Fletcher *et al.*, 2006; Langbein *et al.*, 2005, 2006; Liu *et al.*, 2006) indicate a moment of the earthquake of 10^{18} N m (**M** 6.0). The earthquake nucleated beneath Gold Hill at a depth of 7.9 km and ruptured for about 20 km in a direction N43°W from Gold Hill. Slip increased to the northwest with a maximum value of 40–50 cm just to the northwest of the town of Parkfield. Inversions of strong-motion data (Fletcher *et al.*, 2006; Liu *et al.*, 2006) also indicate slip primarily to the northwest of the hypocenter but somewhat shallower than that obtained from geodetic and strain data (Langbein *et al.*, 2005). Joint inversion (Dreger *et al.*, 2004; Chen *et al.*, 2004) indicates a compromise slip distribution with a moment of 1.1×10^{18} N m.

This article concerns preseismic, coseismic, and postseismic magnetic field data observed by the array shown in Figure 1. In short, there are no clear short-term magnetic precursors to this earthquake consistent with the absence of measurably strain, pore pressure, and microseismicity precursors (Bakun *et al.*, 2005). Coseismic changes were apparently generated by earthquake-related stress release and indicate a piezomagnetic source (Stacey and Johnston, 1972), rather than an electrokinetic source dependent on crustal fluid flow for these effects (Ishido and Mizutani, 1981).

Longer-term changes during the 30-year period leading up to the earthquake show possible accelerated stressing of the region since 1993. Furthermore, there are no clear ULF

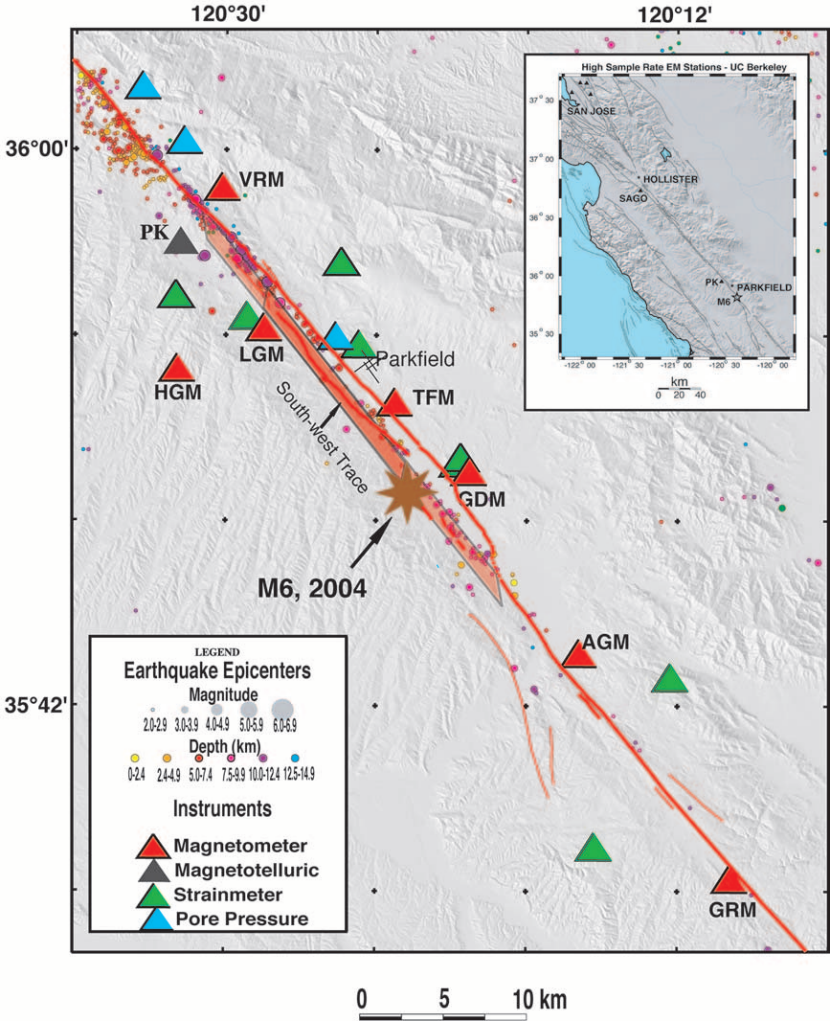

Figure 1. Location of the seven USGS absolute magnetometer sites relative to the epicenter (large star) and rupture (thick box with darkest section showing the greatest slip) of the 28 September, 2004 Parkfield earthquake and its subsequent aftershocks. Also shown is the University of California–Berkeley bandlimited (0.001–10 Hz) magnetic and electric (EM) field monitoring site at the northern end of the rupture (PK) and further up the fault (SAGO). Location of the San Andreas fault trace follows the work of Rymer *et al.* (2006). Also shown for reference are borehole strainmeter and pore pressure sites.

electromagnetic signals that occurred before or after the earthquake at the monitoring point PK within a kilometer or so of the earthquake rupture, although magnetic field and electric field seismograms were registered at the time of the earthquake probably because of ground displacement and tilting produced by the earthquake seismic waves.

Instrumentation

The U.S. Geological Survey has been operating a time-synchronized network of seven absolute proton precession magnetometers in the Parkfield region of the San Andreas fault since 1976 (Fig. 1) with network completion in 1985. The purpose of this network is to quantify the form and character of local magnetic fields along active faults preceding and during fault rupture. Due to budget cutbacks, network maintenance has been decreased in recent years, but at the time of the 2004 **M** 6.0 Parkfield earthquake, all systems were operating. At the PK site, Frank Morrison, Sierra Boyd, and others from the University of California–Berkeley, have installed a three-component very broadband magnetic induction coil system (EMI-Schlumberger) together with two (100 m and 200 m) horizontal orthogonal electric dipole pairs. PK is within a few kilometers of the northwestern extent of the surface rupture on the fault for this earthquake. This magnetic system is capable of recording magnetic field change over the band 0.0001 Hz to 20 Hz with noise amplitude less than 2 pT/(√Hz) This band overlaps that for which Fraser-Smith *et al.* (1990) reported recording high magnetic noise prior to the Loma Prieta earthquake. Electric field noise in the same band is less than 50 μV/km in the uncorrected data. Most importantly, a similar site was also installed at SAGO, a UC Berkeley geophysical monitoring site on the San Andreas fault some 80 km to the northwest along the fault. This allows identification and correction for common-mode noise at the PK site due to disturbances in the ionosphere/magnetosphere.

Most total field sites, particularly GH located immediately above the earthquake hypocenter, are within the near field (i.e., a few rupture lengths) of the earthquake. All total field sites operate at 0.25 *nT* sensitivity. Data are synchronously sampled every 10 min and transmitted with Geostationary Operation Environmental Satellite (GOES) digital satellite telemetry to the U.S. Geological Survey (USGS) at

Menlo Park, California, for processing (Mueller *et al.*, 1981). All sensors are mounted at about 2 m above the ground within deeply cemented wooden posts. Sites were chosen for maximum expected signal amplitude in locations where spatial magnetic gradients at the sensors are less than 1 nT/m to avoid spurious signals from sensor movement during earthquakes. The sites are also at distances of several kilometers from the fault where spurious signals cannot be caused by the large-scale displacement of magnetic material on the other side of the fault during earthquakes and fault slip.

Short-Term Data

To isolate magnetic field changes of local origin and to reduce common mode noise from ionospheric and magnetospheric sources some few hundred kilometers above the sites, we difference data from adjacent sites. The standard deviation σ of hourly means of the resulting difference field data increases with site separation as

$$\sigma = a + bd, \tag{1}$$

where $a = 0.07 \pm 0.08$ nT, $b = 0.01 \pm 0.003$ nT/km, and d is the site separation in kilometers (Johnston *et al.*, 1984). Figure 2a shows the differenced data for station VRM minus TFM for the two weeks before and 11 days after the Parkfield earthquake. Raw data values and the same data with 83-point smoothing applied before and after the earthquake are shown in the upper and lower plots, respectively. The difference in absolute field offsets at the two magnetometer sites is 0.4 ± 0.1 in the 83-point smoothed data. Figure 2b shows these same data for all the different site pairs. Clear offsets are apparent on many of the station pairs. In this figure, and a time expanded view in Figure 2c, it is also apparent that unusual magnetic field changes above the noise levels did not occur in the 10-min sampled data during the hours to minutes before the earthquake.

Short-term magnetic field differences of 0.4 nT or so are not uncommon in magnetic difference field data taken with site separations of between a few kilometers to 20 km. Changes of this amplitude occur frequently during magnetic disturbances, solar flares, and solar storms and arise largely from differences in magnetic induction at the two sites. Adaptive filtering techniques can reduce these signals (Davis

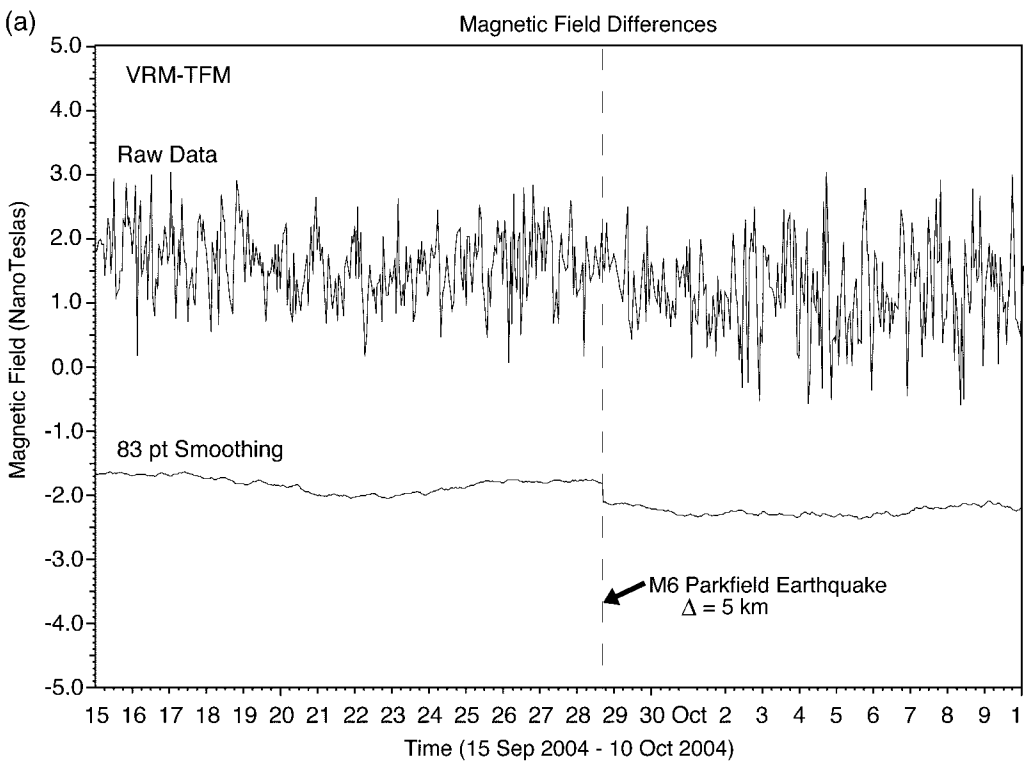

Figure 2. (a) Magnetic field differences between VRM and TFM from 15 September to 10 October 2004 covering the time of the **M** 6.0 28 September 2004 Parkfield earthquake showing 1h samples (upper plot), same data with 83-point smoothing before and after the earthquake (lower plot). All data are displayed with identical vertical scale. Δ indicates the distance to the earthquake rupture. (b) Magnetic field differences between all site pairs from 15 September to 10 October 2004 covering the time of the **M** 6.0 28 September 2004 Parkfield earthquake. All data are displayed with identical vertical scale in nT. (c) Expanded version of the difference field data for the week leading up to the earthquake. (*continued*)

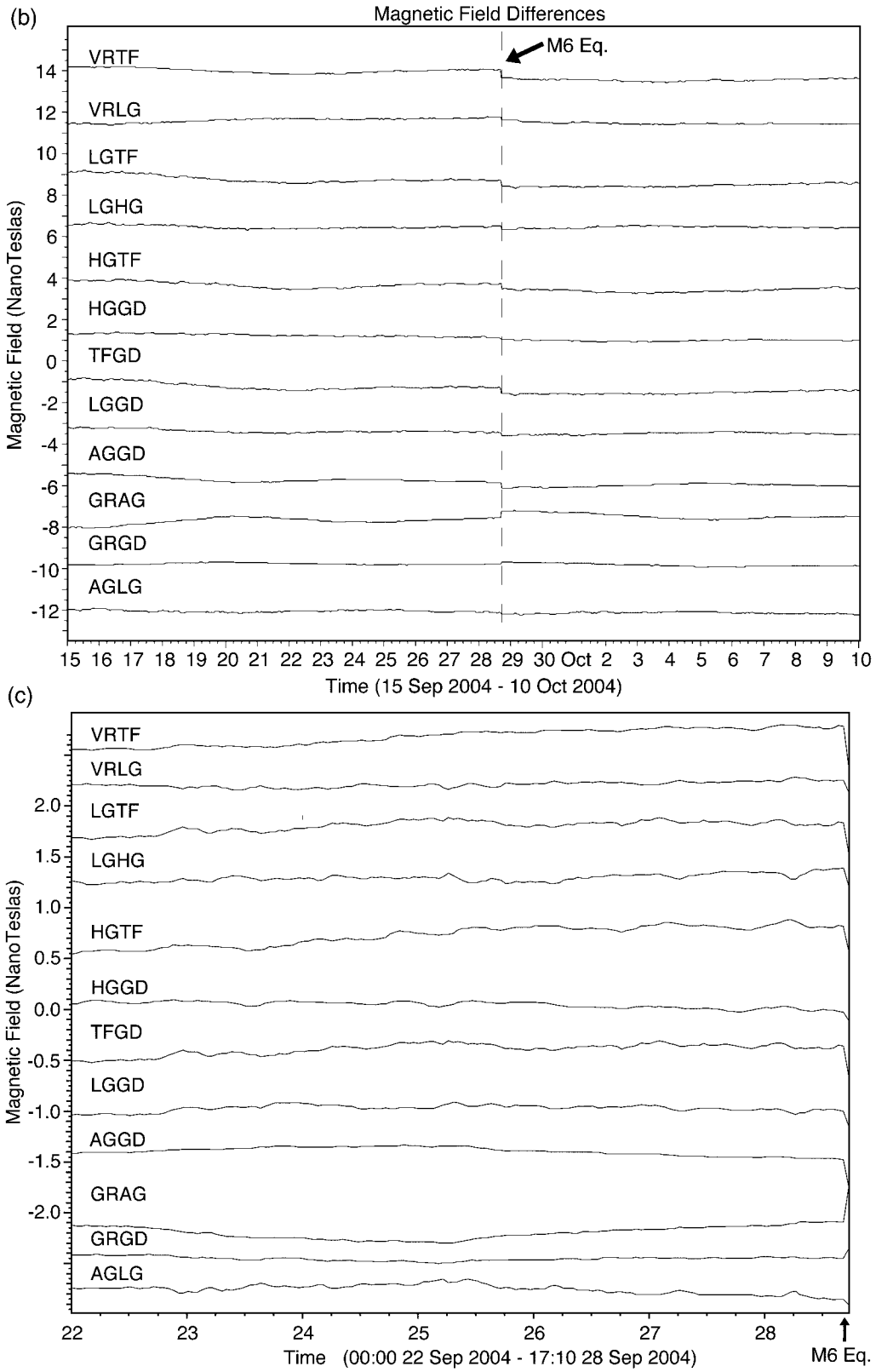

Figure 2. Continued.

and Johnston, 1983). Fortunately, the solar activity during the 24-hr before and after the Parkfield earthquake was quiet, and the changes coincident with the earthquake at 17:15 UTC on 28 September cannot easily be ascribed to external magnetic disturbance effects since these do not generate permanent offsets.

Determination of the actual coseismic offsets at each site from the difference field offsets is not straightforward since all sites are close to the earthquake. The nearest magnetometers of similar design and synchronized sampling times are located in Long Valley caldera, some 217 km to the northeast. The 95% confidence limits ($\pm 2\sigma$) of continuous hour averages of difference field data from the Parkfield sites are expected from equation (1) to be 2.1 $\pm$ 0.6 nT. To obtain finer resolution of the offsets we further processed the difference data sets during the month before and after the earthquake. We rejected all data for days in which magnetic disturbances occurred and all data during daytime hours when S_q disturbances are evident. Linear regression fits were then made to the remaining nighttime values during the month before and the month after the earthquake, and the offsets were determined. The errors are the sum of the standard errors of variation about each regression line and are approximately equal to the 95% confidence limits. Other techniques were used in attempt to determine actual offsets. These included (1) calculating all differences with respect to a particular site chosen to be a reference (AGM) and (2) determining a network mean and differencing all data to that mean. While these techniques have lower offset errors, both suffer from the possibility that all the resulting offset data may be biased. This bias can be determined using the Long Valley data, and the measurements of the observed offsets are listed in Table 1 and shown as a function of position in Figure 3.

Table 1

Magnetic Field Offsets Recorded at the Various Sites as a Result of the 28 September 2004 **M** 6.0 Parkfield Earthquake

Site	Latitude	Longitude	Magnetic Field Offset (nT)
GDM	35.8420	−120.3380	+0.3
AGM	35.7371	−120.2490	+0.1
GRM	35.6022	−120.1640	+0.2
TFM	35.8651	−120.3820	−0.4
VRM	35.9788	−120.5100	−0.1
LGM	35.9062	−120.4760	+0.1
HGM	35.8850	−120.5570	+0.2

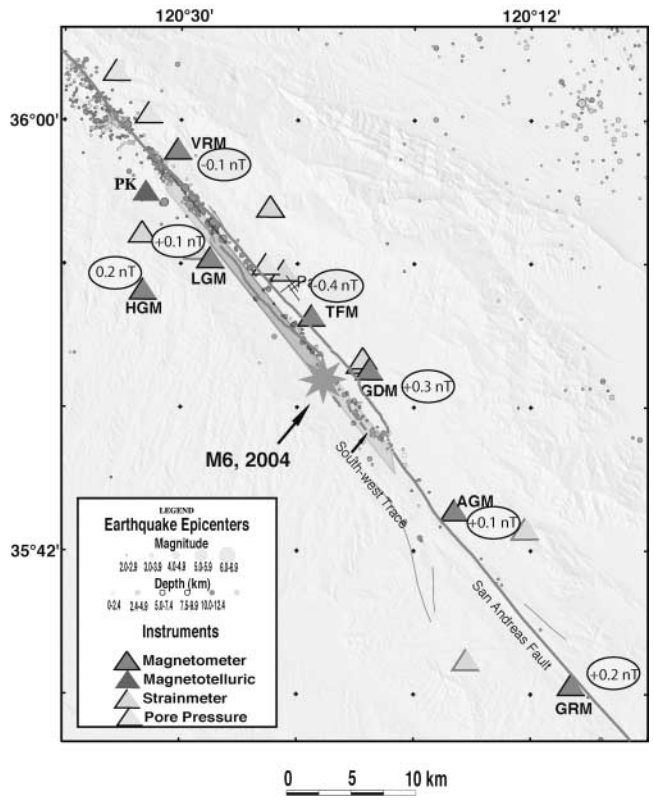

Figure 3. Observed offsets shown as a function of site for the **M** 6.0 2004 Parkfield earthquake.

Long-Term Data

Longer-term plots of smoothed difference data from the different site pairs for the 18 years before the earthquake are shown in Figure 4a after correction for normal secular variation at these sites (Johnston *et al.*, 1985). It is apparent that changes in both magnetic field rate at several sites and magnetic field transients at others occurred from 1993 to the present. These field changes occurred at the same time as changes in strain, displacement, microseismicity, and three **M** 4.0–5.0 earthquakes (Gwyther *et al.*, 1996; Langbein *et al.*, 1999). The magnetic field rate changes have similar form to the changes in strain and fault slip, as shown in the comparative plot in Figure 4b. Since a 7-year drought in the Parkfield region also broke in 1993, it is possible that the strain and displacement data may have resulted from strain related near-surface hydrologic effects (Langbein *et al.*, 1999). However, the occurrence of three **M** 4–5 events in 1992, 1993, and 1994—the largest earthquakes on this section of fault since the 1966 **M** 6.0 earthquake—could not be a result of rainfall. Nor would rainfall cause magnetic changes with the same form as the strain and displacement changes.

It might be questioned whether these long-term magnetic field changes might be somehow related to the 11-year solar activity cycle or the result of differential induction effects of higher-order secular variation in the geomagnetic field. The solar activity peaked in 1990 and again in 2001 (Hathaway, 2006). There are no corresponding disturbances in the magnetic record during these times. Rather, 1993 to 1997 is the least active time in the solar cycle. Furthermore, if magnetic disturbance activity is a contributing factor, this would not explain the strain, displacement, and seismicity data. Thus, taking all the data sets together, it seems likely

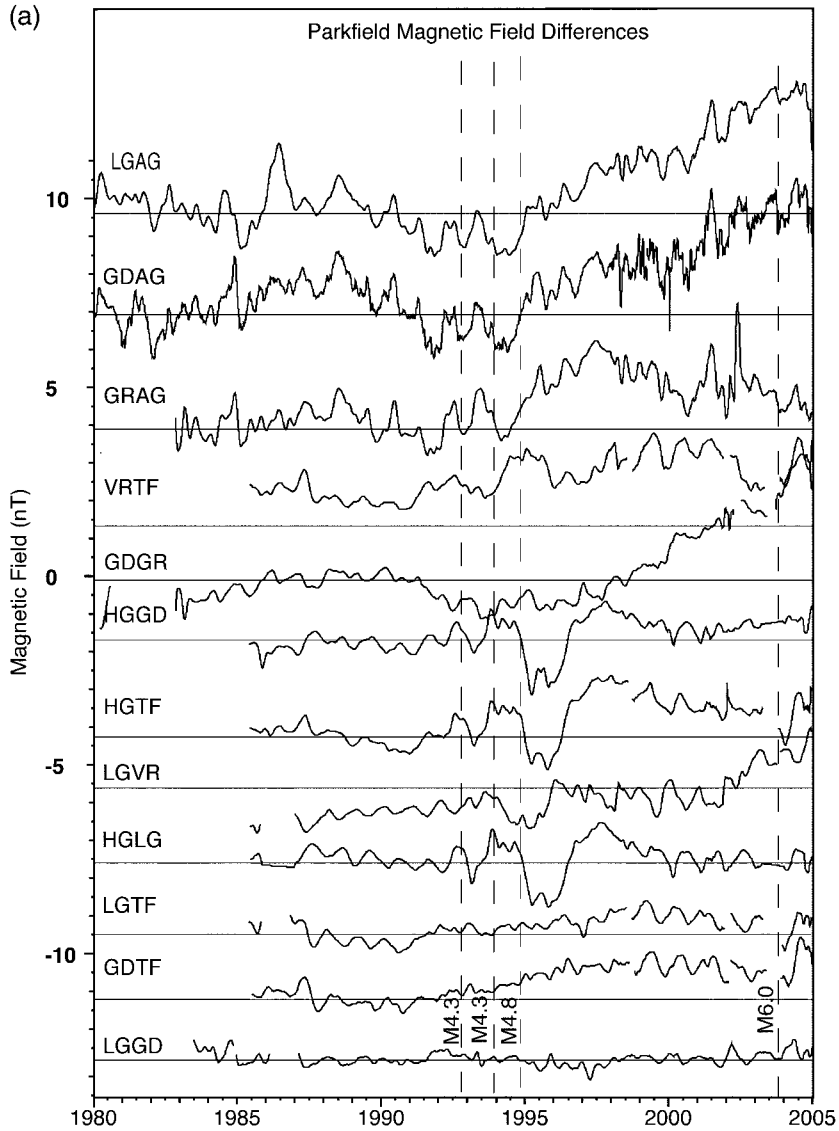

Figure 4. (a) Longterm magnetic difference data from 1980 to the present showing indications of rate change in the early 1990s. These data are corrected for secular variation as discussed in Johnston *et al.* (1985). (b) Comparative strain, displacement, and fault slip from Langbein *et al.* (1999) and magnetic field difference from LGM and AGM on the same timescale. (*continued*)

that they have a generally common or related source. It is more difficult to determine whether higher-order secular variation effects are somehow leaking into the data since we need knowledge of the magnetic susceptibility distribution and long-term magnetic component data in the region. Again, the correspondence with strain, displacement, and fault slip would suggest that this is not the case.

To determine the long-term magnetic field changes at the various magnetometer sites, we have processed the data in the same manner as discussed above for the coseismic offsets. The offset data are listed in Table 2 and are shown as a function of position in Figure 5. If Figure 3 and Figure 5 are compared, it is immediately apparent that the longer-term changes are generally opposite in sign, particularly in the south, and larger in amplitude than those produced by the earthquake as would be expected from the longer-term loading rate in the region (Savage *et al.*, 1987).

ULF Data

Figure 6 shows plots of PK data after these data have been corrected using a prediction transfer function from similar data at SAGO and bandpassed to cover the band 0.01–20 Hz where precursory EM signals have been suggested to occur preceding earthquakes (Fraser-Smith *et al.*, 1990; Kopytenko *et al.*, 1993). With regard to the electric field measurements, no indications of electric field (SES) events of the type reported by VAN (Varotsos *et al.*, 1993a, b) are evident in the raw data or, more importantly, in the cleaned bandpassed data. We note that SES events of 25 mV/km, comparable to those reported by Varotsos *et al.* (1993a, 1993b), would be readily observed in these data. Future use of adaptive filtering techniques will eventually reduce the noise even further.

Increased noise is also not apparent in either the raw or cleaned/bandpassed magnetic field data shown in Figure 6

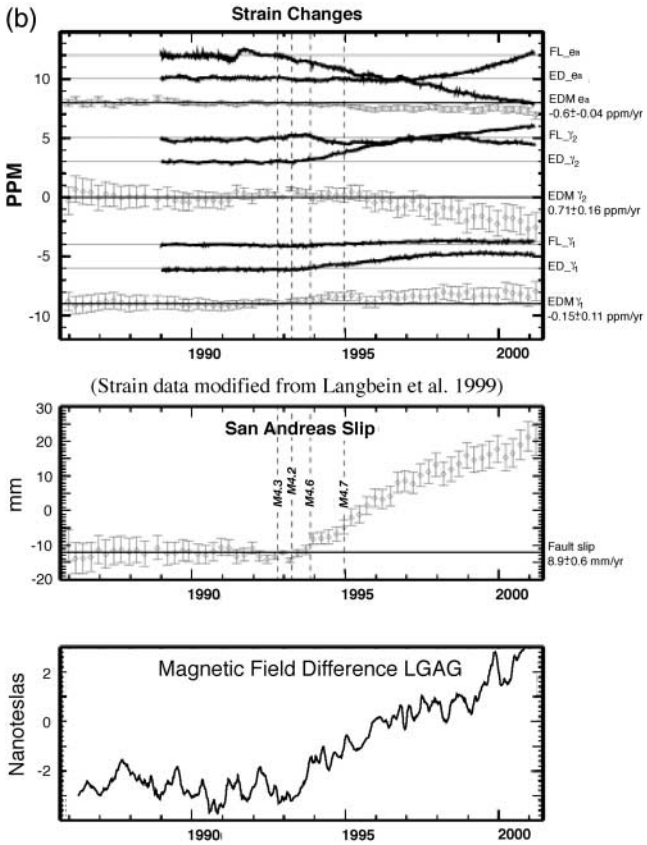

Figure 4. Continued

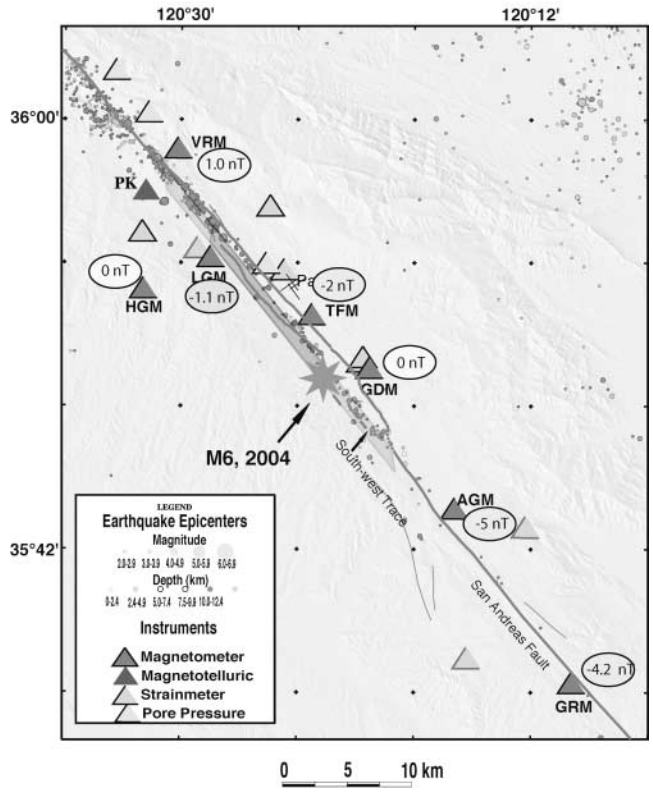

Figure 5. Observed long-term offsets shown as a function of site from 1987 to the present.

Table 2
Magnetic Field Offsets Recorded at the Various Sites since 1993

Site	Latitude	Longitude	Magnetic Field Offset (nT)
GDM	35.8420	−120.3380	+0.0
AGM	35.7371	−120.2490	−5.0
GRM	35.6022	−120.1640	−4.2
TFM	35.8651	−120.3820	−1.8
VRM	35.9788	−120.5100	+1.0
LGM	35.9062	−120.4760	−1.1
HGM	35.8850	−120.5570	+0.0

during the period of days to minutes before the earthquake as reported by Fraser-Smith *et al.* (1990) for the **M** 7.1 Loma Prieta earthquake and by Kopytenko *et al.* (1993) for the 1988 Spitak **M** 6.9 earthquake. The results at PK are very important since (1) the recordings are within a few kilometers of the edge of the rupture similar to the sensor/rupture position for the Loma Prieta earthquake and definitely much closer than 120–200 km as in the case of the Spitak earthquake; (2) the instrumentation has very low noise; and (3) corrections can be made for external common-mode noise from the ionosphere/magnetosphere. Thus, a direct near-field check of the type and form of EM signals occurring prior to, during, and following earthquakes of this magnitude can be made. The 96% confidence levels for north–south and east–west electric fields during this period from 24 September to 29 September are 13.3 μV/km and 28.2 μV/km while the 95% confidence levels for north–south, east–west, and vertical magnetic fields during the same period are are 19.2 pT, 63.2 pT, and 14.0 pT. For comparison, the magnetic signals claimed by Fraser-Smith *et al.* (1990) to be related to the Loma Prieta earthquake without correction for magnetic and ionospheric noise were about 1 nT—some 50 times larger.

We also searched the data from PK before and after the earthquake and at other times of similar solar activity for indications of increased noise. For this analysis, noise amplitude spectra were computed from 26.6-min sections of data during the preearthquake and postearthquake periods and also during similar consecutive 26.6-min periods at other times. No significant differences in noise amplitude spectra were observed in the data before and after the earthquake. Figure 7 shows a plot of noise amplitude spectra as a function of time for the 10 days before and after the earthquake using data that has first been corrected for common-mode signals predicted from SAGO. Note that noise amplitude signals of the form reported by Fraser-Smith *et al.* (1990) would be more than an order of magnitude larger than the values presented here. Other noise reduction tech-

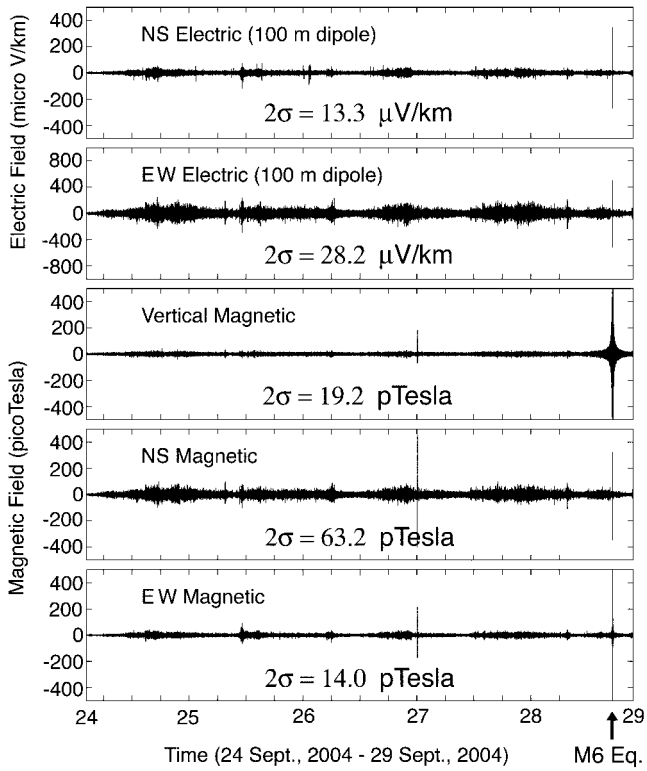

Figure 6. Components of high-frequency electric and magnetic field from PK as a function of time for the 5 days preceding the **M** 6.0 2004 Parkfield earthquake after these data have been corrected using a prediction transfer function from similar data at SAGO and bandpassed to cover the band 0.01–20 Hz where precursory EM signals have been suggested to occur preceding earthquakes (Fraser-Smith *et al.*, 1990; Kopytenko *et al.*, 1993).

niques will also be applied to these data in the future (Kappler *et al.*, 2005).

Correspondence between seismograms from comparative ground strain, ground displacement, ground velocity, and acceleration at sites near PK and magnetic and electric field seismograms at PK for the 30 sec before and after the earthquake indicates that a large part of the electric and magnetic field seismograms are likely produced by electromagnetic induction as a result of ground displacement and tilting of the electrodes and magnetic coils within the Earth's magnetic field by the earthquake shaking (Honkura *et al.*, 2004).

Discussion

Coseismic magnetic field offsets observed for the September 2004 Parkfield earthquake are expected to result from seismomagnetic effects since both the induced and the remanent magnetization are sensitive to the change in crustal stress produced by the earthquake (Nagata, 1969; Sasai, 1980, 1991, Stacey, 1964; Stacey and Johnston, 1972). It is less likely that these rapid and irreversible changes in magnetic field could result from electrokinetic (EK) effects—electromagnetic fields resulting from earthquake-induced pore fluid flow changes (Dobrovolsky *et al.*, 1989, Fitterman, 1979; Ishido and Mizutani, 1981; Mizutani *et al.*, 1976) since this would require rapid and implausibly continuous fluid flow. Expected EK signals would likely be short-term transients with temporally decaying magnetic signals such as observed in water-well records near the fault rupture. There was no indication of fluid flow from the ground at any point along the surface rupture, nor was there any permanent change in pore pressure or water-well level (Johnston *et al.*, 2005a, b). Thus, while the EK mechanism cannot be discounted, a more obvious explanation in terms of the piezomagnetic effect seems likely.

Following the methods described in Sasai (1980, 1991) and Johnston and Mueller (1987), a seismomagnetic model of the 2004 Parkfield earthquake was constructed from fault models based on inversion of offsets in borehole strain and GPS displacements for both uniform slip (Johnston *et al.*, 2005a,b) and variable slip (Langbein *et al.*, 2005, 2006). Other models are derived from joint inversion of GPS and strong-motion data (Chen *et al.*, 2004) and inversion of just the strong-motion data (Liu *et al.*, 2006). Since observations of surface magnetization at the various sites ranged between 2.0 A/m and 0.1 A/m and since magnetization usually increases below the weathered near-surface rocks, an average magnetization of 2 A/m was assumed. A stress sensitivity of 2×10^{-5} MPa^{-1}, consistent with theoretical calculations (Stacey and Johnston, 1972) and conservative values of laboratory measurements (Martin, 1980; Revol *et al.*, 1977) were chosen. Using each of these models, shown in cross section in Figure 8, magnetic field perturbations were calculated for a magnetic field inclination and declination of 60° and 15°, respectively. All parameters used are listed in Table 3. The uniform slip model (Fig. 9a) gave some general agreement in sign and observed field values but tended to overestimate the observations in the south and underestimate the observations near the northern end and middle (TF, GH) of the rupture. Much better agreement was obtained with the Langbein *et al.* (2006) variable slip model (Fig. 9b), most likely since higher slip is concentrated to the northwest of the hypocenter. Poorer agreement was found with the Chen *et al.* (2004) model (Fig. 9c) where, again, slip is concentrated to the northwest of the hypocenter but it is deeper. The worst fit was to the Lui *et al.* (2006) model for which substantial shallow slip is proposed to the north of the 1966 **M** 6.0 earthquake. This model would also not be consistent with the GPS data. At this stage, none of the models provide

Table 3
Parameters Used in Piezomagnetic Model

Sensitivity K (MPa^{-1})	Magnetization (A/m)	Incl.	Decl.	Curie Depth (km)
0.0002	2	60°	15°E	15

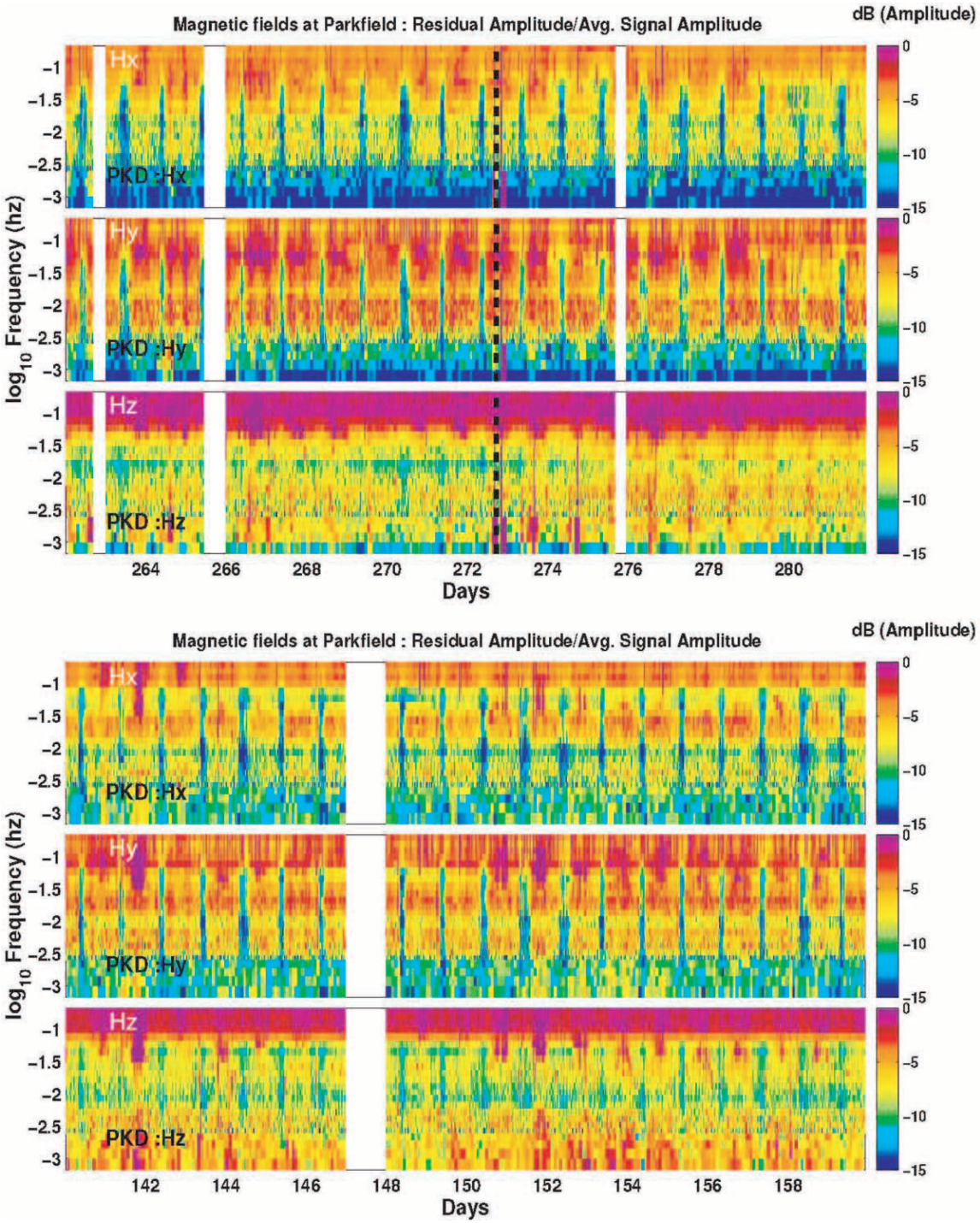

Figure 7. Magnetic field amplitude spectra (frequency band 0.01 Hz to 1 Hz) as a function of time for the 5 days before the **M** 6.0 2004 Parkfield earthquake (upper) compared with the background noise amplitude spectra during magnetic noise normal times (lower).

exact agreement and none fit the strong field gradient between GDM and TFM. This gradient is perhaps suggestive of shallower slip on the fault in this region. Clearly, joint inversion of all data (geodetic, strong motion, and magnetic) could provide a better estimate of the slip distribution. Because of model uncertainties, particularly slip distribution, magnetization distribution, and stress sensitivity, agreement should not be expected to better than 50% since uniform magnetization was assumed. Future models will include variable magnetization determined from local anomaly maps

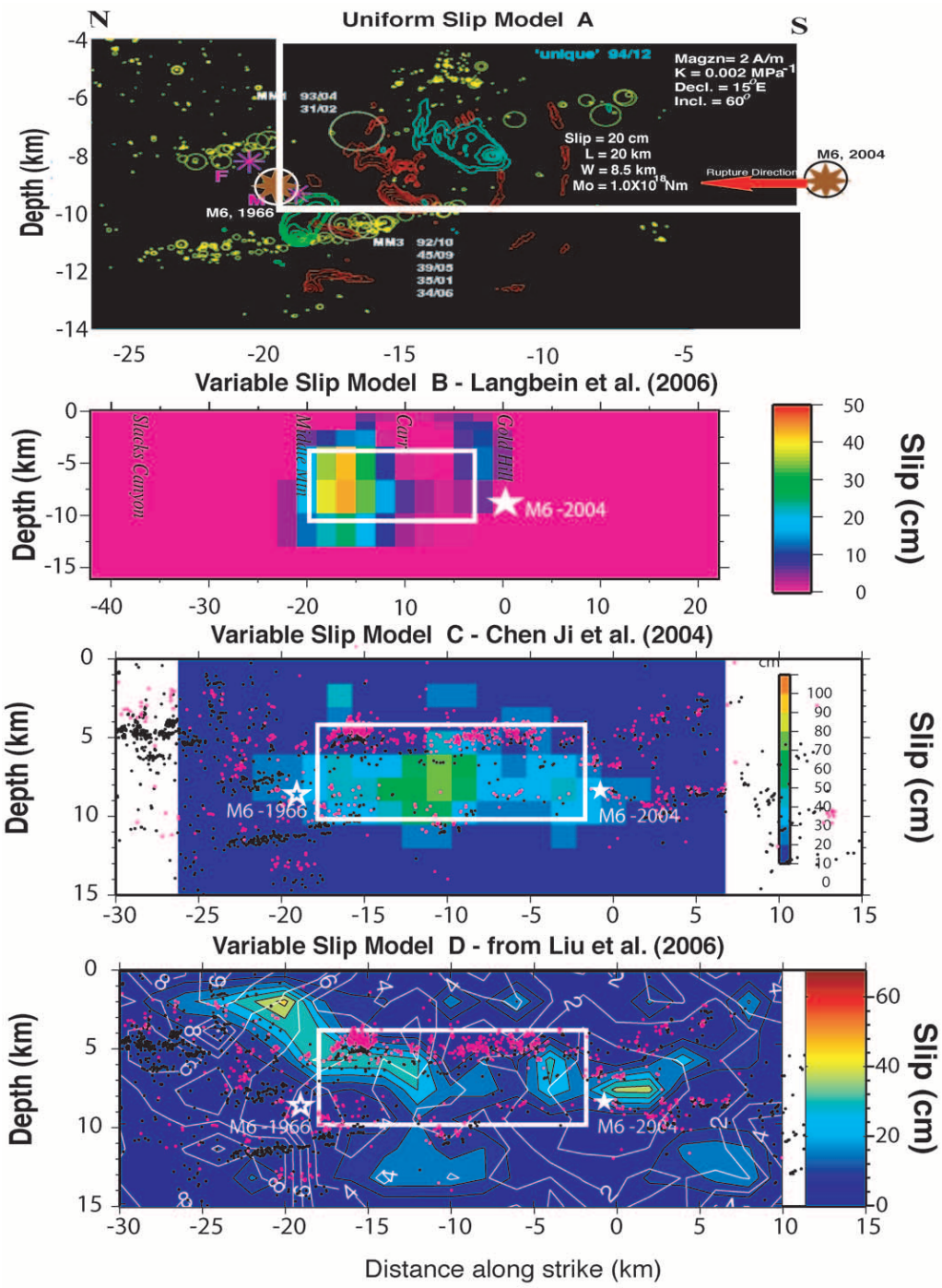

Figure 8. Slip cross section for the **M** 6.0 Parkfield earthquake from inversion of Global Positioning System (GPS) and strain data for a uniform slip model A, inversion of GPS data for a variable slip model B, from Langbein *et al.* (2006), inversions of GPS and strong-motion data in a variable slip model C from Chen *et al.* (2004) and inversion of strong-motion data in a variable slip model D from Liu *et al.* (2006). For reference, the uniform slip model is included on each of the variable slip models. The background for model A is from Fletcher and Spudich (1998). Fault parameters for model A are listed on the cross section. Fault parameters for model B (Langbein *et al.*, 2006), model C (Chen *et al.*, 2004), and model D (Liu *et al.*, 2005) used to model the event are listed in the respective papers.

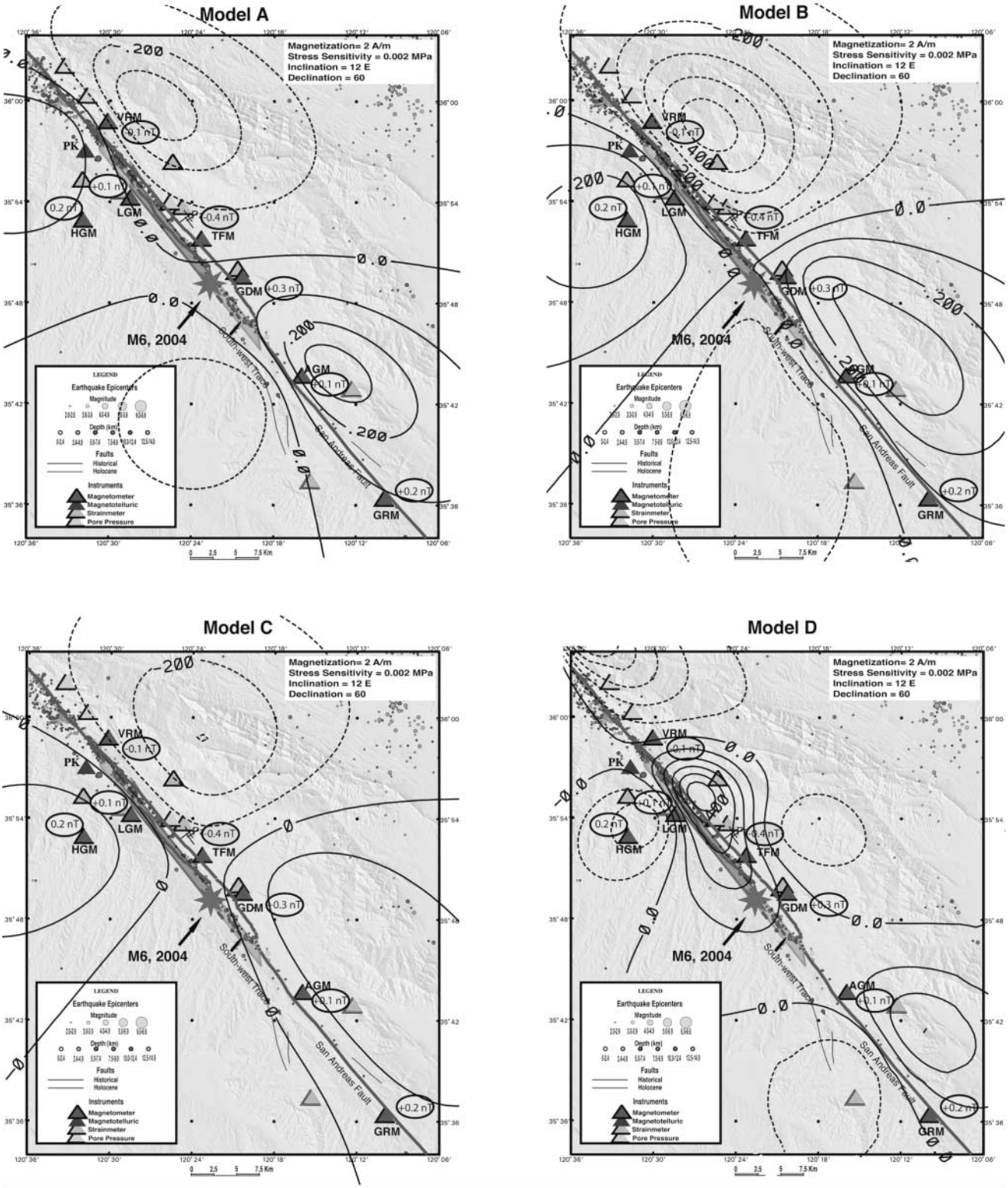

Figure 9. Contours of calculated magnetic field (nT) expected from the 2004 Parkfield earthquake for four slip models (A, B, C, and D). Seismomagnetic model parameters are listed in Table 3. Contour interval is 0.1 nT.

and improved estimates of slip distribution on the fault. The absence of clear postseismic magnetic changes is not unexpected since the magnetic data are sensitive to elastic behavior produced by changes in stress and less sensitive to anelastic behavior associated with postseismic slip. Furthermore, smaller longer-term signals are more difficult to identify in these magnetic data.

The longer-term changes in local magnetic fields in the Parkfield region are intriguing. They are generally opposite in sense and much larger, particularly in the south, than the changes produced by the earthquake. These changes would be consistent with increased loading within the creep-locked transition zone produced by accelerated slip beneath the region starting in the early 1990s. This may have triggered the increased shear strain and moderate seismicity during this time, but the moderate seismicity and perhaps associated limited slip are insufficient to produce the observed changes in magnetic field, particularly at sites up to 20 km away in the southeast.

We have generated a magnetic loading model (albeit poorly constrained) of the entire creeping-to-locked transition region. This model is similar though larger than the earthquake stress drop model discussed above. To generate the observed changes of up to 4 *nT* over the 10-year period would require substantially more stress accumulation than was released in the 2004 **M** 6.0 Parkfield. This would imply that the Parkfield earthquake did not release all accumulated stress in the region as indicated also by the large postseismic slip that followed the earthquake (Langbein *et al.*, 2006). The earthquake moment release and postseismic moment release was equivalent to at least two **M** 6.0 earthquakes. At the current loading rate of 33 mm/yr (Savage *et al.*, 1987), slip equivalent to a **M** 6.4 earthquake should be expected on each 20-km segment of fault every 20 years. The details are further complicated by the likelihood that the great 1857 **M** 8 Fort Tejon earthquake that ruptured the San Andreas fault from Parkfield to San Bernardino released only 3 m of slip on the Chalome fault segment (Sieh and Jahns, 1984) and thus did not completely release the stress on this segment. A high stress gradient therefore should be expected on the segment to the south of Gold Hill, and changes in this gradient may be what we are seeing on the long-term magnetic data. As others (Harris and Archuleta, 1988, Sieh and Jahns, 1984) have speculated, a larger earthquake propagating to the southeast into the Chalome segment is likely in the future.

Conclusions

Static magnetic field decreases of as much as 0.4 *nT* occurred at monitoring sites immediately surrounding the rupture of the 18 September 2004 **M** 6.0 Parkfield earthquake. These were similar in amplitude to those recorded during the larger **M** 7.3 1992 Landers earthquake (Johnston *et al.*, 1994) and the more comparable 8 July 1986 M_L 5.9 North Palm Springs earthquake (Johnston and Mueller, 1987). These coseismic seismomagnetic effects most likely result from stress-induced reversible changes in magnetization (piezomagnetic effects) and less likely result from electric currents caused by earthquake-driven fluid flow (EK effects). Rupture-driven charge generation in a crust with a conductivity of 1–10 S/m are unlikely to contribute to this process. Electrokinetic effects would require long-term continuous fluid flow at seismogenic depths to explain the magnetic field offsets. The absence of surface or subsurface indications of major fluid flow in strain and pore pressure data argues against the likelihood of an EK mechanism at Parkfield. The observations presented here are thus most consistent (in both amplitude and sense) with a simple piezomagnetic model of the earthquake. This model has as its essence the same general fault-slip geometry, slip amplitudes, and earthquake moment that can be used to explain the seismic and geodetic ground displacement data generated by the earthquake.

No significant changes in local magnetic field occurred in the weeks to minutes before the earthquake on any of the seven synchronized magnetometers in the region. This is consistent with the absence of changes in strain, pore pressure, microseismicity, ground displacement, and electric field during this time (Bakun *et al.*, 2005, Langbein *et al.*, 2005) Nor were changes in magnetic and electric field in the ULF band observed during this time on the PK magnetotelluric monitoring system operated by the University of California–Berkeley. This raises further questions concerning whether the changes observed by Fraser-Smith *et al.* (1990) and Kopytenko *et al.* (1993) were really related to the earthquakes that followed. The PK system is a high-quality low-noise EM monitoring system, and a second system SAGO at distance of about one ionospheric height further up the fault allows correction for external electromagnetic disturbances. The PK system is within a few kilometers of the end of the earthquake rupture, yet no increased EM noise was observed. The only potentially significant difference was the smaller size of the Parkfield earthquake compared to the **M** 7.1 Loma Prieta earthquake. However, larger earthquakes do not imply larger stress changes (drops) only larger total slip and rupture length (Aki and Richards, 1980), and PK is close to the end of the eventual rupture where stress changes are greatest.

No electric field disturbances of the form proposed by Varotsos *et al.* (1993a, b) and Nagao *et al.* (1996) to precede earthquakes were observed above the instrument noise on the various electrodes. This noise level is more than an order of magnitude below the signals reported by Varotsos *et al.* (1993a, b).

A higher rate of longer-term magnetic field change, consistent with increased loading in the region, is apparent since 1993. This accompanied an increased rate of secular shear strain, observed on a two-color geodimeter network and a small network of borehole tensor strainmeters, and increased seismicity dominated by three **M** 4.5–5.0 earthquakes that occurred roughly a year apart in 1992, 1993, and 1994. Models incorporating all of these data indicate increased slip at depth in the region. Accelerated loading may have played a

role in the final occurrence of the 28 September 2004 **M** 6.0 Parkfield earthquake, but the details are not at all clear.

Acknowledgments

We thank Paul Davis and Yoshi Honkura for insightful reviews and Frank Morrison and Karl Kappler of UC Berkeley for providing the EM data from site PK and details of the measurement system. We thank John Langbein and Pengcheng Liu for details of their respective slip models. We also thank Rich Leichti, Andy Snyder, Doug Myren, and Vince Keller for helping with instrument maintenance and Jonathan Glen and Darcy McPhee for reviewing the article.

References

Aki, K., and P. G. Richards (1980). *Quantitative Seismology: Theory and Methods*, Freeman and Co, San Francisco, 932 pp.

Bakun, W. H., B. Aagaard, B. Dost, W. L. Ellsworth, J. L. Hardebeck, R. A. Harris, M. J. S. Johnston, J. Langbein, J. J. Lienkaemper, A. J. Michael, J. R. Murray, R. M. Nadeau, P. A. Reasenberg, E. A. Roeloffs, A. Shakal, R. W. Simpson, and F. Waldhauser (2005). Implications for prediction and hazard assessment from the 2004 Parkfield Earthquake, *Nature* **437,** 969–974.

Bernard, P. (1992). Plausibility of long distance electrotelluric precursors to earthquakes, *J. Geophys. Res.* **97,** 17,531–17,546.

Chen, Ji, K. K. Choi, N. King, K. M. Larsen, and K. W. Hudnut (2004). Co-seismic slip history and early afterslip of the 2004 Parkfield earthquake (2004). *EOS Trans. AGU* **85,** no. 47, Fall Meeting Suppl. (S53D-04 abstract).

Davis, P. M., and M. J. S. Johnston (1983). Localized geomagnetic field changes near active faults in California 1974-1980, *J. Geophys. Res.* **88,** 9452–9460.

Davis, P. M., D. D. Jackson, and M. J. S. Johnston (1980). Further evidence of localized geomagnetic field changes before the 1974 Thanksgiving Day earthquake, Hollister, California, *Geophys. Res. Lett.* **7,** 513–516.

Dobrovolsky, I. P., N. I. Gershenzon, and M. B. Gokhberg (1989). Theory of electrokinetic effects occurring at the final stage in the preparation of a tectonic earthquake, *Phys. Earth Planet. Interior* **57,** 144–156.

Dreger, D., M. H. Murray, and D. Oglesby (2004). Kinematic modeling of the 2004 Parkfield Earthquake, *EOS Trans. AGU* **85,** no. 47, Fall Meeting Suppl., S51C–0170I (abstract).

Egbert, G. D., M. Eisel, O. S. Boyd, and H. F. Morrison (2000). DC trains and Pc3s: source effects in mid-latitude geomagnetic transfer functions, *Geophys. Res. Lett.* **27,** 25–28.

Fitterman, D. V. (1979). Theory of electrokinetic-magnetic anomalies in a faulted half-space, *J. Geophys. Res.* **84,** 6031–6041.

Fletcher, J. B., and P. Spudich (1998). Rupture characteristics of the three M ~ 4.7 (1992-1994) Parkfield earthquakes, *J. Geophys. Res.* **103,** 835–854.

Fletcher, J. B., P. Spudich, and L. M. Baker (2006). Direct observation of earthquake rupture propagation in the 2004 Parkfield, California, earthquake using the UPSAR accelerograph, *Bull. Seism. Soc. Am.* **96,** no. 4B, S129–S142.

Fraser-Smith, A. C., A. Bernardi, P. R. McGill, M. E. Ladd, R. A. Helliwell, and O. G. Villard, Jr (1990). Low-frequency magnetic field measurements near the epicenter of the M_L 7.1 Loma Prieta earthquake, *Geophys. Res. Lett.* **17,** 1465–1468.

Fraser-Smith, A. C., P. R. McGill, R. A. Helliwell, and O. G. Villard, Jr. (1994). Ultralow-frequency magnetic field measurements in southern California during the Northridge earthquake of January 17, 1994, *Geophys. Res. Lett.* **21,** 2195–2198.

Gwyther, R. L., M. T. Gladwin, and R. H. G. Hart (1996). Anomalous tensor strain at Parkfield during 1993-1994, *Geophys. Res. Lett.* **23,** 2425–2428.

Harris, R. A., and R. J. Archuleta (1988). Slip budget and potential for a M 7 in central California, *Geophys. Res. Lett.* **15,** 1215–1218.

Hathaway, D. H. (2006). Sunspot cycle predictions, http://science.msfc.nasa.gov/ssl/pad/solar/predict.html (last accessed July 2005).

Hayakawa, M. (1999). *Atmospheric and Ionospheric Phenomena Associated with Earthquakes*, Terra Scientific Publishing Co., Tokyo, 996 pp.

Hayakawa, M., R. Kawate, O. A. Molchanov, and K. Yumoto (1996). Results of ultra-lowfrequency magnetic field measurements during the Guan earthquake of 8 August, 1993, *Geophys. Res. Lett.* **23,** 241–244.

Honkura, Y., H. Sato, and Y. Ogawa (2004). Seismic dynamo effects associated with the M7.0 earthquake of 26 May 2003 off Miyagi Prefecture and the M6.2 earthquake in northern Miyagi Prefecture, NE Japan, *Earth Planets Space* **56,** 109–114.

Ishido, T., and H. Mizutani (1981). Experimental and theoretical basis of electrokinetic phenomena in rock-water systems and its application to geophysics, *J. Geophys. Res.* **86,** 1763–1775.

Johnston, M. J. S. (1989). Review of magnetic and electric field effects near active faults and volcanoes in the U.S.A., *Phys. Earth Planet. Interiors* **57,** 47–63.

Johnston, M. J. S., and R. J. Mueller (1987). Seismomagnetic observation with the July 8, 1986, M_L 5.9 North Palm Springs earthquake, *Science* **237,** 1201–1203.

Johnston, M. J. S., R. D. Borcherdt, M. Gladwin, D. Myren, M. Mee, G. Glassmoyer, and C. Dietel (2005a). High-resolution strain on the San Andreas fault at Parkfield before, during, and after the September 28, 2004 Parkfield Earthquake: implications for fault response, nucleation, earthquake prediction, and tremor, *Seism. Res. Lett.* **76,** 217.

Johnston, M. J. S., R. D. Borcherdt, A. Linde, and M. Gladwin (2005b). Continuous borehole strain and pore pressure in the near-field of the September 28, 2004 **M** 6.0 Parkfield earthquake: implications for nucleation, fault response, earthquake prediction, and tremor, *Bull. Seism. Soc. Am.* **96,** no. 4B, S56–S72.

Johnston, M. J. S., R. J. Mueller, and Y. Sasai (1994). Magnetic field observations in the near-field of the June 18, 1992, M_w 7.3 Landers, California, earthquake, *Bull. Seism. Soc. Am.* **84,** 792–798.

Johnston, M. J. S., R. J. Mueller, R. H. Ware, and P. M. Davis (1984). Precision of geomagnetic measurements in a tectonically active region, *J. Geomag. Geoelec.* **36,** 83–95.

Johnston, M. J. S., S. A. Silverman, R. J. Mueller, and K. Breckenridge (1985). Secular variation, crustal sources and tectonic activity in California, 1976–1984, *J. Geophys. Res.* **90,** 8707–8717.

Kappler, K., F. Morrison, and G. Egbert (2005). Long-term monitoring of EM signals near Parkfield, CA, *EOS Trans. AGU* **86,** no. 52, Fall Meeting Suppl. T51B-1345, (abstract).

Karakelian, D., G. C. Beroza, S. L. Klemperer, and A. C. Fraser-Smith (2002). Analysis of ultralow frequency electromagnetic field measurements associated with the 1999 M7.1 Hector Mine earthquake sequence, *Bull. Seism. Soc. Am.* **92,** 1513–1524.

Kopytenko, Y. U. A., T. G. Matiashvili, P. M. Veronov, and O. A. Molchanov (1993). Detection of ultra-low frequency emissions connected with the Spitak earthquake and its aftershock activity, based on geomagnetic pulsation data at Dusheti and Vardzia, *Phys. Earth Planet. Interiors* **77,** 85–95.

Langbein, J., R. Borcherdt, D. Dreger, J. Fletcher, J. L. Hardebeck, M. Hellweg, Ji Chen, M. Johnston, J. R. Murray, R. Nadeau, M. Rymer, and J. Treiman (2005). Preliminary report on the 28 September 2004, M 6.0 Parkfield, California earthquake, *Seism. Res. Lett.* **76,** 10–26.

Langbein, J., R. Gwyther, R. Hart, and M. Gladwin (1999). Slip rate increase at Parkfield in 1993 detected by high-precision EDM and borehole tensor strainmeters, *Seism. Res. Lett.* **26,** 2529–2532.

Langbein, J., J. R. Murray, and H. A. Snyder (2006). Coseismic and initial postseismic deformation from the 2004 Parkfield California earthquake, observed by GPS, creepmeters, and borehole strainmeters, *Bull. Seism. Soc. Am.* **96,** no. 4B, S304–S320.

Liu, P., S. Custodio, and R. Archuleta (2006). Kinematic inversion of the 2004 **M** 6.0 Parkfield earthquake including site effects, *Bull. Seism. Soc. Am.* **96,** no. 4B, S143–S158.

Martin, R. J., III (1980). Is piezomagnetism influenced by microcracks during cyclic loading, *J. Geomag. Geoelec.* **32,** 741–755.

Mizutani, H., T. Ishido, T. Yokokura, and S. Ohnishi (1976). Electrokinetic phenomena associated with earthquakes, *Geophys. Res. Lett.* **13,** 365–368.

Mueller, R. J., and M. J. S. Johnston (1990). Seismomagnetic effect generated by the October 18, 1989, M_L 7.1 Loma Prieta, California, earthquake, *Geophys. Res. Lett.* **17,** 1231–1234.

Mueller, R. J., M. J. S. Johnston, B. E. Smith, and V. G. Keller (1981). U.S. Geological Survey magnetometer network and measurement techniques in Western U.S.A., *U.S. Geol. Surv. Open-File Report 81-1346*.

Nagao, T., S. Uyeda, Y. Asai, and Y. Kono (1996). Anomalous Changes in Geoelectric Potential Preceding Four Earthquakes in Japan, in *A Critical Review of VAN—Earthquake Prediction from Seismic Electric Signals*, Sir J. Lighthill (Editor) World Scientific, Singapore, 292–300.

Nagata, T. (1969). Basic magnetic properties of rocks under the effect of mechanical stresses, *Tectonophysics* **21,** 427–445.

Park, S. K., M. J. S. Johnston, T. R. Madden, F. D. Morgan, and H. F. Morrison (1993). Electromagnetic precursors to earthquakes in the ULF band: a review of observations and mechanisms, *Rev. Geophysics* **31,** 117–132.

Park, S. K. (1997). Monitoring resistivity change in Parkfield, California, *J. Geophys. Res.* **102,** 24,545–24,559.

Parrot, M. (1994). Statistical study of ELF/VLF emissions recorded by a low-altitude satellite during seismic events, *J. Geophys. Res.* **99,** 339–347.

Pham, V. N., D. Boyer, G. Chouliaras, J. L. Le Mouel, J. C. Rossignol, and G. N. Stavrakakis (1998). Characteristics of electromagnetic noise in the Ioannina region (Greece): a possible origin for so-called seismic electric signals (SES), *Geophys. Res. Lett.* **25,** 2229–2232.

Revol, J., R. Day, and M. Fuller (1977). Magnetic behavior of magnetite and rocks stressed to failure—relation to earthquake prediction, *Earth Planet. Sci. Lett.* **37,** 296–306.

Rymer, M. J., T. C. Tinsley, J. A. Treiman, J. R. Arrowsmith, K. B. Clahan, A. M. Rosinski, W. A. Bryant, H. A. Snyder, G. S. Fuis, N. Toke, and G. W. Bawden (2006). Surface fault slip associated with the 2004 Parkfield, California, earthquake, *Bull. Seism. Soc. Am.* **96,** no. 4B, S11–S27.

Sasai, Y. (1980). Application of the elasticity theory of dislocation to tectonomagnetic modeling, *Earthquake Res. Inst. Bull.* **55,** 387–447.

Sasai, Y. (1991). Tectonomagnetic modeling on the basis of linear piezomagnetic theory, *Earthquake Res. Inst. Bull.* **66,** 585–722.

Savage, J. C., W. H. Prescott, and M. Lisowski (1987). Deformation along the San Andreas fault 1982–1987 as indicated by frequent Geodolite measurements *J. Geophys. Res.* **92,** 4785–4797.

Sieh, K. E., and R. M. Jahns (1984). Holocene activity on the San Andreas fault at Wallace Creek, California, *Geol. Soc. Am. Bull.* **1984,** 2283–2395.

Smith, B. E., and M. J. S. Johnston (1976). A tectonomagnetic effect observed before a magnitude 5.2 earthquake near Hollister, California, *J. Geophys. Res.* **81,** 3556–3560.

Stacey, F. D. (1964). The seismomagnetic effect, *Pure Appl. Geophys.* **58,** 5–22.

Stacey, F. D., and M. J. S. Johnston (1972). Theory of the piezomagnetic effect in titanomagnetic-bearing rocks, *Pure Appl. Geophys.* **97,** 146–155.

Varotsos, P., K. Alexopoulos, and M. Azaridou (1993a). Latest aspects of earthquake prediction in Greece based on seismic electric signals, II, *Tectonophysics* **224,** 1–38.

Varotsos, P., K. Alexopoulos, M. Lazaridou-Varotsov, and T. Nagao (1993b). Earthquake predictions issued in Greece by seismic electric signals since February 6, 1990, *Tectonophysics* **224,** 269–288.

U.S. Geological Survey ms977
345 Middlefield Road
Menlo Park, California 94025
(M.J.S.J.)

Disaster Prevention Division
Tokyo, Metropolitan Government
Tokyo 113, Japan
(Y.S.)

Oregon State University
Corvallis, Oregon 97331
(G.E.)

UNAVCO
6350 Nautilus Drive
Boulder, Colorado 80301
(R.J.M.)

Manuscript received 15 September 2005.